Convergence behaviour of different formulations for time-harmonic and transient eddy-current computations in 3D

D. van Riesen, C. Kaehler and G. Henneberger

Abstract: Several different formulations for the calculation of eddy-currents using the finite-element method have been proposed. For 3D applications in static cases the magnetic vector potential with edge elements is the most common case. The static formulation can be extended to account for eddy-current effects using an additional term with the same magnetic vector potential with an electric vector potential or with an electric scalar potential. The last is commonly believed to be the best in terms of stability and convergence rate. This paper considers the three different formulations in a time-harmonic and a transient case for a simple C-core model and the TEAM Workshop problem 7. The effects of time and space discretisation are analysed. The TEAM Workshop problem is also verified against measurement results obtained by Fujiwara *et al.*

1 Introduction

Eddy-current calculation in electromagnetic devices is becoming more important as both the available computational power and the need for electric power loss reduction increase. Several different formulations for the calculation of eddy-currents using the finite-element method have been proposed. For 3D applications in static cases the magnetic vector potential $\vec{A}$ with edge elements is the most common case. The static formulation can be extended to account for eddy-current effects using an additional term with the same magnetic vector potential ($\vec{A} - \vec{A}^*$ formulation), with an electric vector potential $\vec{T}(\vec{A} - \vec{A}, \vec{T}$ formulation) or with an electric scalar potential $V(\vec{A} - \vec{A}, V$ formulation). The last is commonly believed to be the best in terms of stability and convergence rate. This paper considers the three different formulations in a time-harmonic and a transient case for a simple C-core model and the TEAM Workshop problem 7 [1]. The effects of time and space discretisation are analysed. The TEAM Workshop problem is also verified against measurement results obtained by Fujiwara *et al* [1]. All the solvers are part of the iMOOSE software package [2, 3].

2 Formulations

A very thorough overview over the above-mentioned formulations for the eddy-current analysis is given by Bíró [4] for the time-harmonic problems. The most simple formulation uses a modified magnetic vector potential $\vec{A}^*$ with the flux density $\vec{B} = \nabla \times \vec{A}^*$ and the electric field $\vec{E} = -j\omega\vec{A}^*$. The resulting Galerkin form using edge basis functions to approximate $\vec{A}^*$ reads

$$\int_\Omega \nabla \times \vec{\alpha}_i \nu \nabla \times \vec{A}^* d\,\Omega + \int_\Omega j\omega\sigma\vec{\alpha}_i \cdot \vec{A}^* d\,\Omega = \int_\Omega \nabla \times \vec{\alpha}_i \cdot \vec{T}_0 d\,\Omega \quad \forall i = 1, 2, \ldots, n_e \tag{1}$$

where Ω is the regarded field domain, $\vec{\alpha}_i$ are vector shape functions, α_i scalar shape functions and ν is the reluctivity. This formulation is suited only for short-circuited eddy-current regions, and is said to have poor numerical stability [4]. Therefore an electric scalar potential V is introduced. It is approximated using nodal basis functions in the elements, requiring a program code capable of mixing nodal and edge element types. The Galerkin form of the system equation is given by

$$\int_\Omega \nabla \times \vec{\alpha}_i \cdot \nu \nabla \times A d\Omega + \int_\Omega j\omega\sigma\vec{\alpha}_i \cdot \vec{A} d\Omega + \int_\Omega j\omega\sigma\vec{\alpha}_i \cdot \nabla V = \int_\Omega \nabla \times \vec{\alpha}_i \vec{T}_0 d\Omega \quad \forall i = 1, 2, \ldots, n_e \tag{2}$$

$$\wedge \int_\Omega j\omega\sigma\nabla\alpha_i \cdot \vec{A} \mathrm{d}\,\Omega + \int_\Omega j\omega\sigma\nabla\alpha_i \nabla V \mathrm{d}\,\Omega = 0 \quad \forall i = 1, 2, \ldots, n_n \tag{3}$$

A formulation using only edge basis functions considers an electric vector potential $\vec{T}$ with the current density $J = \nabla \times \vec{T}$

$$\int_\Omega \nabla\times\vec{\alpha}_i \nu \nabla \times \vec{A} \mathrm{d}\Omega + \int_\Omega \vec{\alpha}_i \nabla \times \vec{T} = \int_\Omega \vec{\alpha}_i \cdot \vec{J}_0 \mathrm{d}\,\Omega \quad \forall i = 1, 2, \ldots, n_e \tag{4}$$

IEE Proceedings online no. 20040950
doi:10.1049/ip-smt:20040950
Paper first received 10th March 2004 and in revised form 5th July 2004. Originally published online: 22nd November 2004

The authors are with the Department of Electrical Machines, Aachen University (RWTH), Schinkelstraße 4, D-52062 Aachen, Germany

$$\int_\Omega j\omega\sigma\nabla\times\vec{\alpha}_i\vec{A} + \int_\Omega \nabla\times\vec{\alpha}_i\nabla\times\vec{T}\mathrm{d}\,\Omega = 0$$
$$\forall i = 1,2,\ldots,n_e \tag{5}$$

This formulation, however, also has some stability issues. Especially for higher frequencies and/or higher conductivities, the convergence is poor [5]. Additionally the implementation in iMOOSE does not allow for multiply-connected eddy-current regions.

For the transient calculation the formulations are extended with the time-dependent values discretised according to the Galerkin scheme, resulting e.g. for the magnetic vector potential in

$$\vec{A}(t) = (1-\Theta)\vec{A}_n + \Theta A_{n+1} \tag{6}$$

$$\Theta = \frac{t-t_n}{t_{n+1}-t_n} = \frac{t-t_n}{\delta t}; \quad 0 \le \Theta \le 1 \tag{7}$$

with $\Theta = 2/3$ *cf.* Zienkiewicz *et al* [6].

All three formulations share a common formulation for noneddy-current regions, which is equal to the static case (with the added time dependency). Therefore it is not displayed here. The $\vec{A}-\vec{A}, V$ formulation in Galerkin form reads in eddy-current regions

$$\begin{aligned}
&\int_\Omega \tau\nabla\times\vec{N}_i\cdot\nu\nabla\times\vec{A}_{n+1}d\,\Omega + \int_\Omega \frac{\sigma}{\Delta t}\vec{N}_i\cdot\vec{A}_{n+1}d\,\Omega \\
&+ \int_\Omega \frac{\sigma}{\Delta t}\vec{N}_i\cdot\nabla V_{n+1}\mathrm{d}\,\Omega = \int_\Omega (\tau-1)\nabla\times\vec{N}_i\cdot\nu\nabla\times\vec{A}_n\mathrm{d}\,\Omega \\
&+ \int_\Omega \frac{\sigma}{\Delta t}\vec{N}_i\cdot\vec{A}_n + \int_\Omega \frac{\sigma}{\Delta t}\vec{N}_i\cdot\nabla V_n\mathrm{d}\,\Omega \\
&+ \int_\Omega \nabla\times\vec{N}_i\cdot(\tau\vec{T}_{0,n+1} + (1-\tau)\vec{T}_{0,n})\mathrm{d}\Omega \quad \forall i = 1.2,\ldots,n_e
\end{aligned} \tag{8}$$

$$\begin{aligned}
&\wedge \int_\Omega \frac{\sigma}{\Delta t}\nabla N_i\cdot\vec{A}_{n+1}\mathrm{d}\Omega + \int_\Omega \frac{\sigma}{\Delta t}\nabla N_i\cdot\nabla V_{n+1}\mathrm{d}\,\Omega \\
&= \int_\Omega \frac{\sigma}{\Delta t}\nabla N_i\cdot\vec{A}_n\mathrm{d}\Omega + \int_\Omega \frac{\sigma}{\Delta t}\nabla N_i\cdot\nabla V_n\mathrm{d}\Omega \\
&\forall i = 1,2,\ldots,n_n
\end{aligned} \tag{9}$$

The $\vec{A}-\vec{A},\vec{T}$ formulation for eddy-current regions in Galerkin form [7] is

$$\begin{aligned}
&\int_\Omega [\tau\nabla\times\vec{N}_i\nu\nabla\times\vec{A}_{n+1} - \tau\vec{N}_i\nabla\times\vec{T}_{n+1}]d\Omega \\
&= \int_\Omega [(\tau-1)\nabla\times\vec{N}_i\cdot\nu\nabla\times\vec{A}_n \\
&\quad - (\tau-1)\vec{N}_i\nabla\times\vec{T}_n + \tau\vec{N}_i\vec{J}_{0n+1} + (\tau-1)\vec{J}_{0n} \\
&\quad + \nabla\times\vec{N}_i\nu(\tau\vec{B}_{rn+1} + (1-\tau)\vec{B}_{rn})]d\,\Omega \\
&\quad \forall i = 1,2,\ldots n_e
\end{aligned} \tag{10}$$

$$\begin{aligned}
&\wedge \int_\Omega \left(\tau\nabla\times\vec{N}_i\cdot\frac{1}{\sigma}\nabla\times\vec{T}_{n+1} + \nabla\times\vec{N}_i\cdot\frac{1}{\Delta t}\vec{A}_{n+1}\right)d\Omega \\
&= \int_\Omega \left((\tau-1)\nabla\times\vec{N}_i\cdot\frac{1}{\sigma}\nabla\times\vec{T}_n + \nabla\times\vec{N}_i\cdot\frac{1}{\Delta t}\vec{A}_n\right)d\,\Omega \\
&\forall i = 1,2,\ldots,n_e
\end{aligned} \tag{11}$$

The $\vec{A},\vec{A}^*$ formulation is not given here as it can be deduced from (8) by suppressing the term with the electric scalar potential.

3 Results

Two different models are used to test the convergence behaviour of the different formulations. A simple C-core with a conducting plate in the yoke and the TEAM Workshop Problem 7, with results verified against the measurements by Fujiwara *et al* [1]. The $\vec{A}-\vec{A},\vec{T}$ formulation as implemented in iMOOSE is not suited for the multiply connected eddy-current region of the TEAM problem and does not converge for realistic conductivity values in the case of the claw pole alternator. A comparison between the $\vec{A}-\vec{A}^*$ and $\vec{A}-\vec{A},\vec{T}$ formulations was performed by the authors in [5].

3.1 TEAM Workshop problem 7

This problem is a linear quasisteady eddy-current problem with multiconnectivity. It is suited to be simulated with both the time-harmonic and the transient model with $\vec{A}-\vec{A}^*$ and

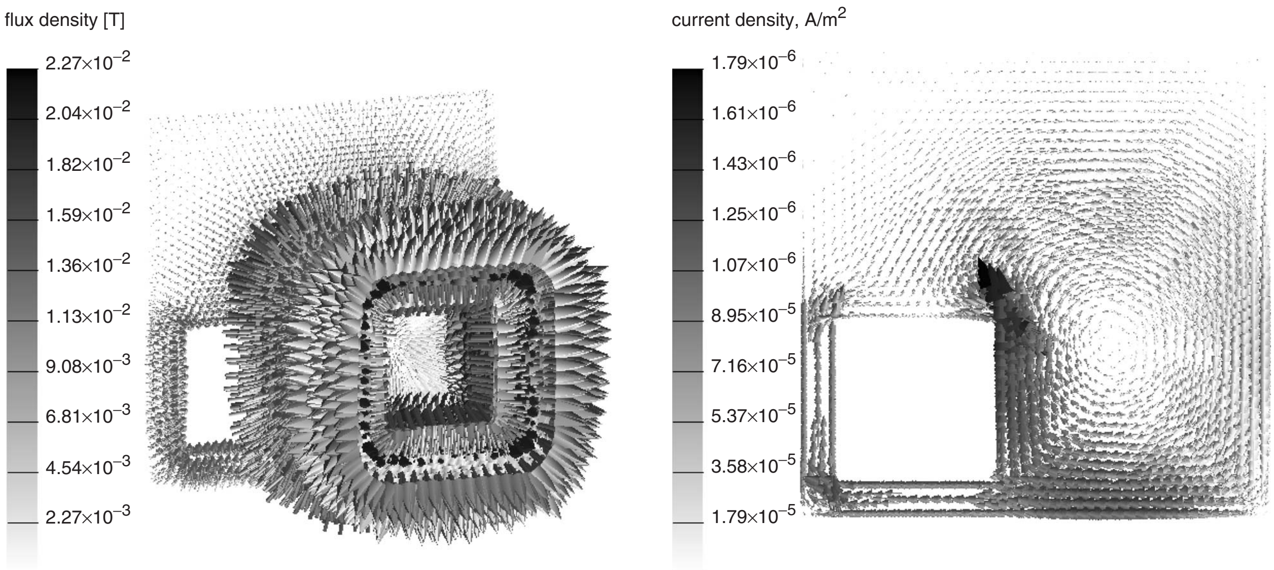

Fig. 1 *Flux density and current density distribution for TEAM Workshop problem 7*

$\vec{A}-\vec{A}, V$ formulations. A sample flux density and current density distribution is depicted in Fig. 1. Reference [1] gives measured values for flux and current density along a sample line in the model. These are compared with the results of the simulation in Fig. 2. Both formulations yield the same results and show a very good agreement with measurements. The model is discretised with various mesh densities, resulting in meshes with 25 000, 50 000, 180 000 and 410 000 first-order tetrahedral, respectively. The number of CG steps required to solve the problem, with the frequency of the exciting current ranging between 10 Hz and 10 kHz, is depicted in Fig. 3*a* for the $\vec{A}-\vec{A}^*$ formulation and in Fig. 3*b* for the $\vec{A}-\vec{A}, V$ formulation. Both formulations are compared for the model with 180 000 elements in Fig. 3*c*. The convergence behaviour evolves as expected. Larger models require more CG steps. For the $\vec{A}-\vec{A}^*$ formulation, a better convergence with ascending frequencies is noted. The $\vec{A}-\vec{A}, V$ formulation requires slightly more CG steps at higher frequencies, although the change is not as pronounced as in the case of the $\vec{A}-\vec{A}^*$ formulation. Figure 4 shows the convergence for the transient model, with three different time steps Δt ($2.5\times10^{-3}s$, $2.5\times10^{-4}s$ and $2.5\times10^{-5}s$, see (7). Due to the computation time required, few frequency samples have been obtained. The differences between the $\vec{A}-\vec{A}^*$ and the $\vec{A}-\vec{A}, V$ formulations are not very pronounced. For the measured case of 50 Hz excitation, Fig. 5 compares the evolution of the residuum of the CG iterations for both the time-harmonic and the transient case. In the time-harmonic model similar oscillations can be noticed with a steeper descent for the $\vec{A}-\vec{A}, V$ formulation, resulting in fewer iteration steps. On the contrary, in the transient model the behaviour is similar for both formulations. This, in addition to the higher number of unknowns resulting from the additional scalar

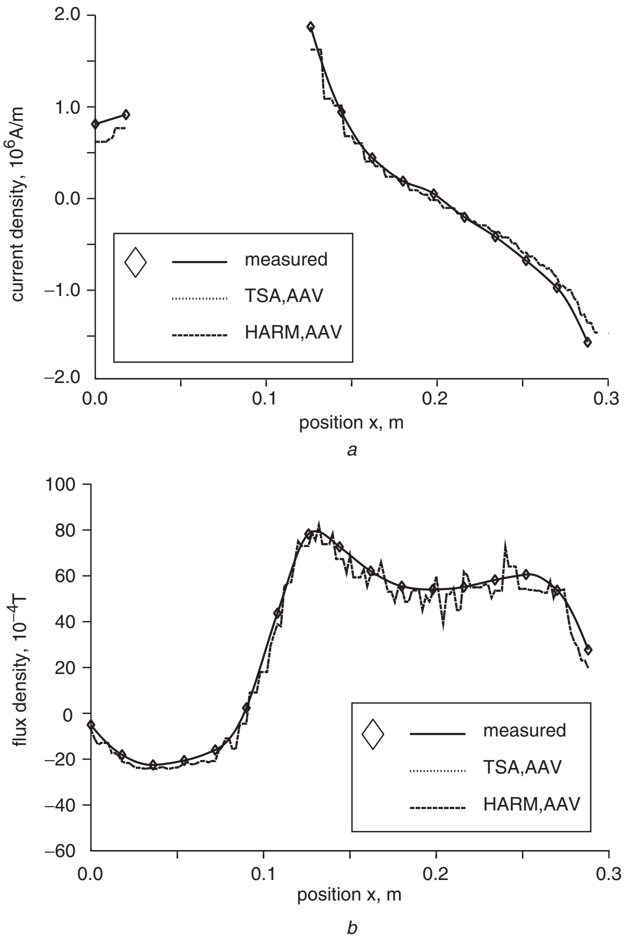

Fig. 2 *Comparison between measured [1] and calculated data for TEAM Workshop problem 7*
a Current density
b Flux density

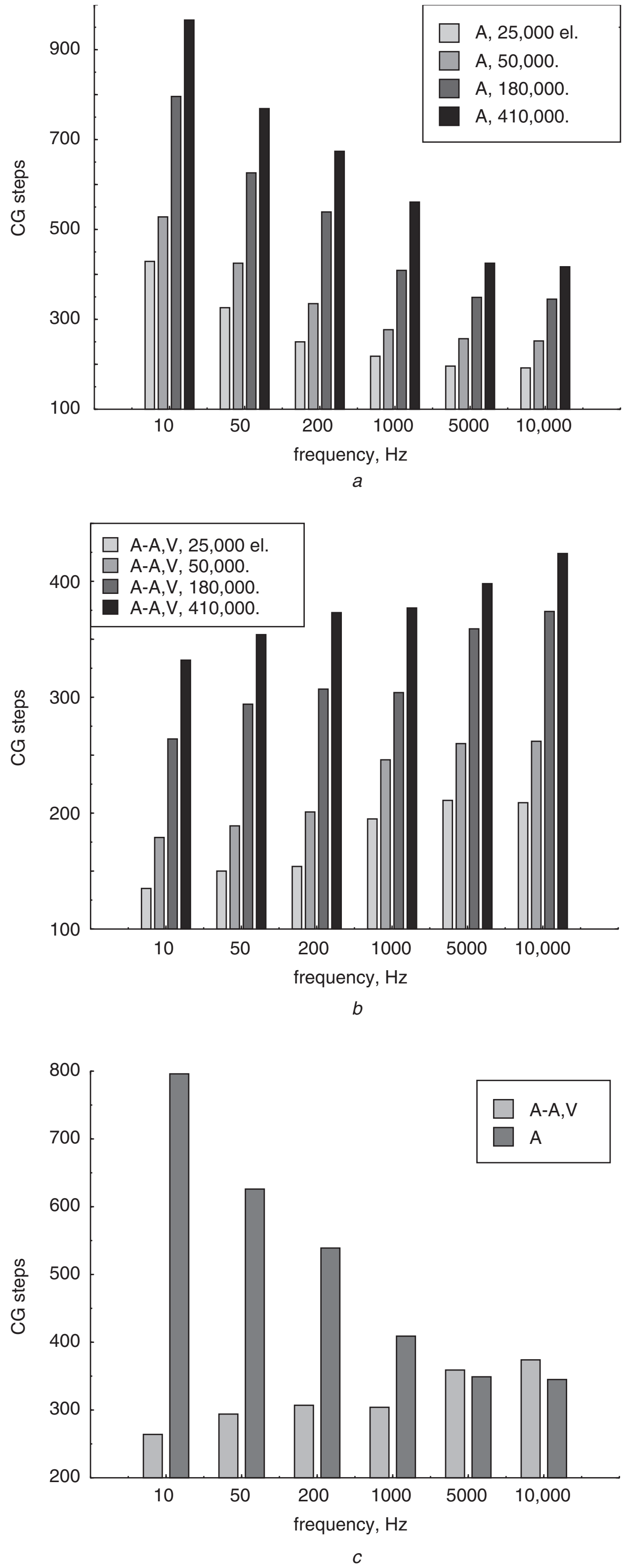

Fig. 3 *Convergence behaviour of TEAM Workshop problem 7, time-harmonic model*
a $\vec{A}-\vec{A}^*$ formulation
b $\vec{A}-\vec{A}, V$ formulation
c Comparison $\vec{A}-\vec{A}^*-\vec{A}-\vec{A}, V$ formulation.

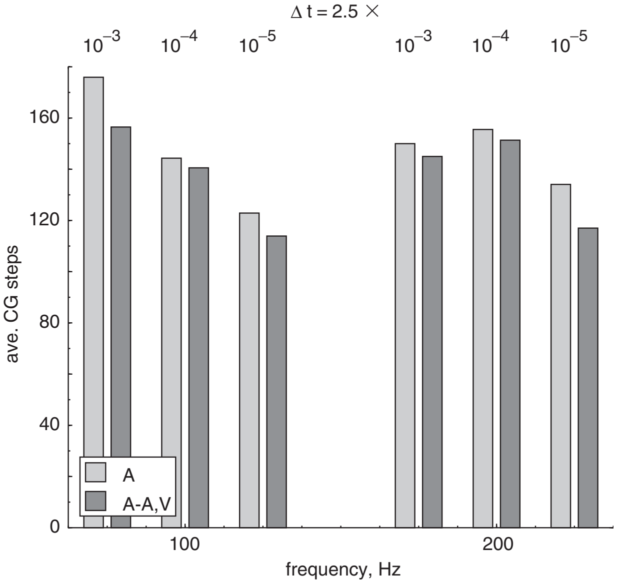

Fig. 4 *Convergence behaviour of TEAM Workshop problem 7, transient model*

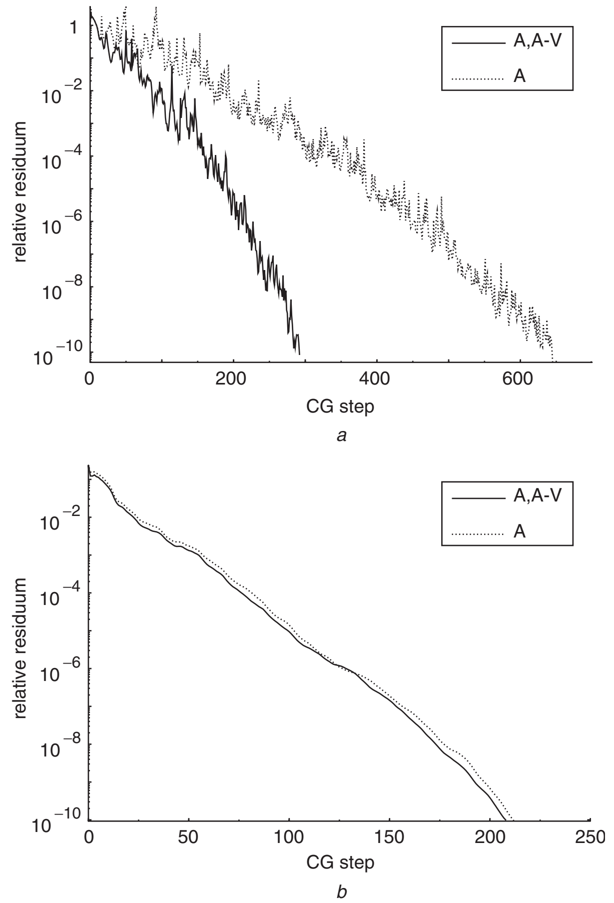

Fig. 5 *Convergence for harmonic and transient calculation of TEAM Workshop problem 7*
a Harmonic
b Transient

potential, results in a higher computation time. Tables 1 and 2 give details about the dimension of the system matrix and the time required for computation.

3.2 Simple C-core

A simple model of a C-core with a conducting region in the yoke and one excitation coil is used for further testing. It is calculated with the time-harmonic and transient model for all three formulations. Figure 6*a* shows the model and Fig. 6*b* the eddy-current distribution in the conducting region for an excitation frequency of 100 Hz. The problem

Table 1: Time, number of CG steps and matrix dimension for time-harmonic problem, TEAM 7

Formulation	Time (s)	Steps	Dim.
$\vec{A}$	1258	645	213,200
$\vec{A}-\vec{A}, V$	800	298	219,864

Table 2: Time, number of CG steps and matrix dimension for transient case, TEAM 7

Formulation	Time (s)	Steps	Dim.
$\vec{A}$	44,882	135	213,200
$\vec{A}-\vec{A}, V$	48,387	140	219,864

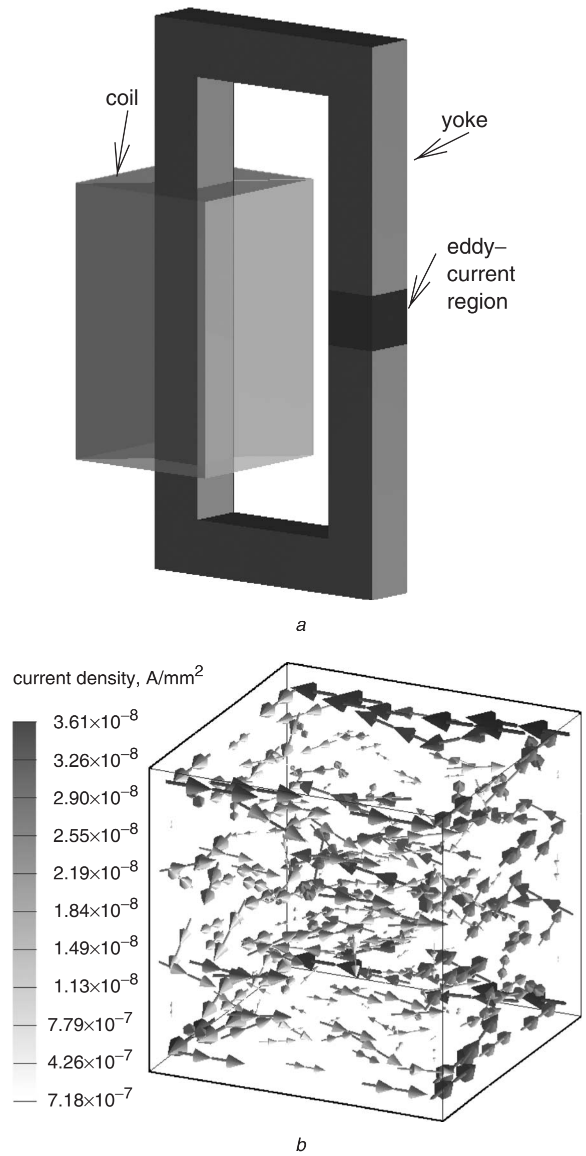

Fig. 6 *Model and eddy-current density solution of simple C-core*
a Model
b Current density

is calculated at different frequencies in the range of 10 to 5000 Hz. Figure 7 shows the number of CG steps needed to reach convergence. Figure 7*a* shows the results for the time-harmonic model. As previously, the convergence for the $\vec{A}-\vec{A}^*$ formulation gets better at higher frequencies. But for the $\vec{A}-\vec{A},\vec{T}$ formulation it gets worse, even such that it does not convergence for 1000 Hz and higher. The $\vec{A}-\vec{A},V$ formulation shows a convergence behaviour that is not significantly affected by the frequency. Figures 7*b* and 7*c* show the transient model. The calculation is performed for three different frequencies with three different time-steps Δt as previously. The $\vec{A}-\vec{A},\vec{T}$ formulation only converges for the larger time-step. The convergence is not affected by the frequency in such a strong way as in the time-harmonic model. The smaller time-steps give better convergence. As opposed to the time-harmonic model, with the smallest time-step there is almost no difference between the $\vec{A}-\vec{A}^*$ and the $\vec{A}-\vec{A},V$ formulation, again resulting in larger computation times for the last. Figure 8 shows a convergence plot for the calculation of the C-core model, both with the time-harmonic (Fig. 8*a*) and the transient (Fig. 8*b*) model. It can easily be seen that the $\vec{A}-\vec{A},\vec{V}$ formulation has larger oscillations in the relative residuum in the CG process, especially for the transient, model. Variations of the preconditioning algorithm have not been performed. Reference [8] showed the effect of preconditioning on the CG convergence characteristics. For the

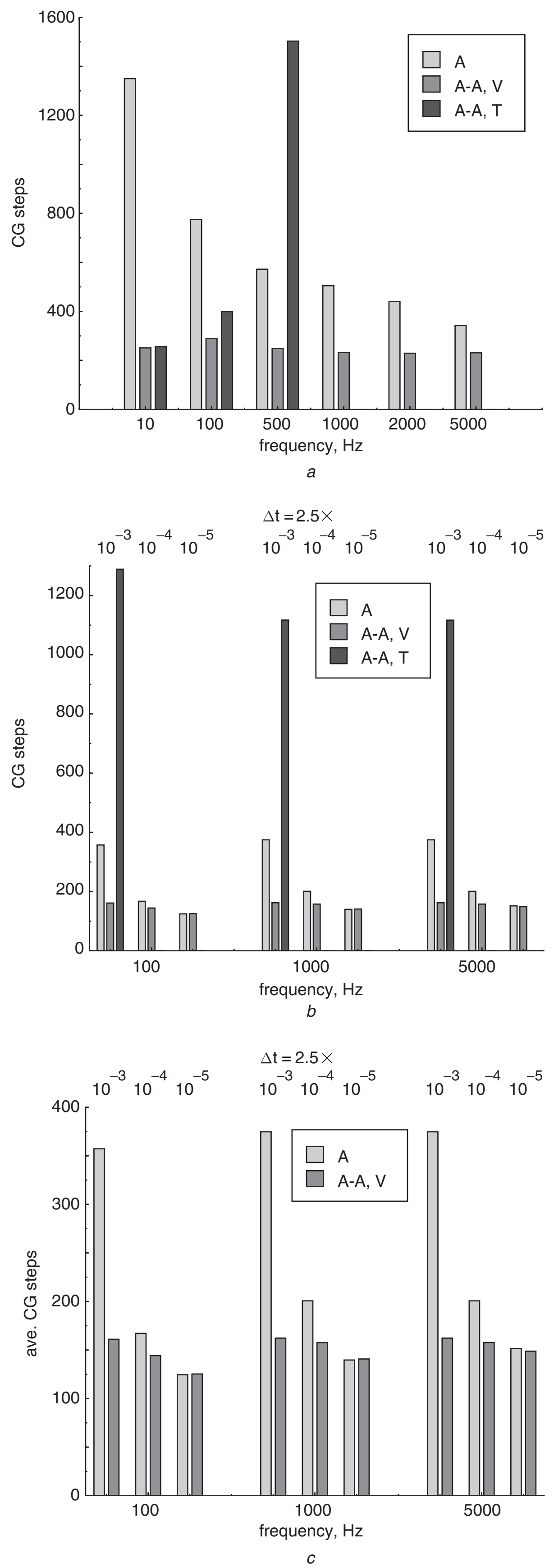

Fig. 7 *Convergence behaviour of C-core*
a Time-harmonic model
b Transient model
c Transient model without $\vec{A}-\vec{A},\vec{T}$ formulation

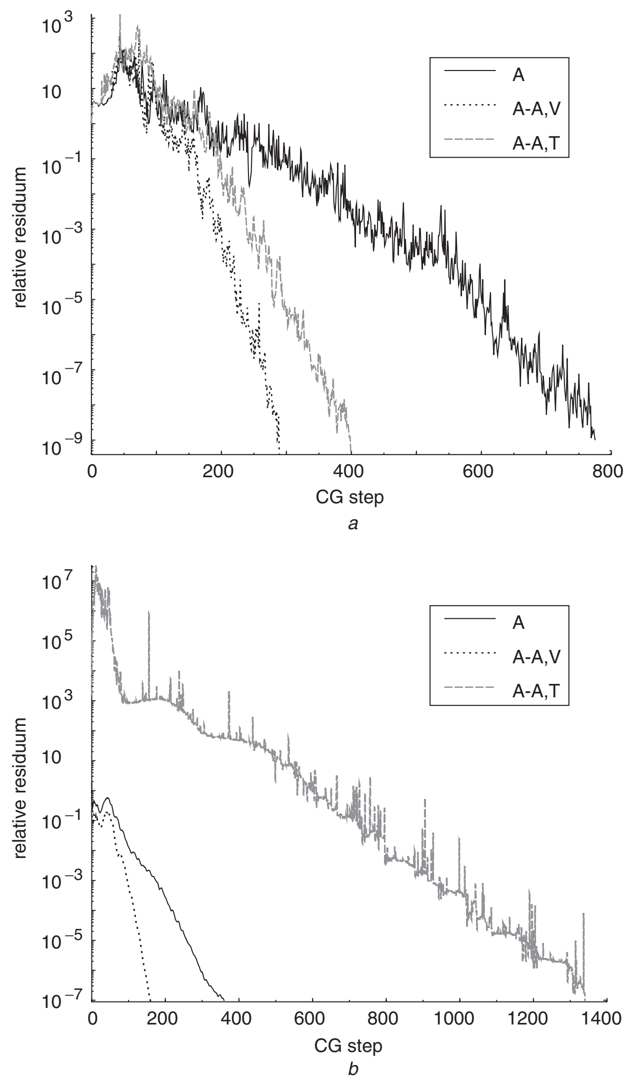

Fig. 8 *Convergence for harmonic and transient calculation of C-core model*
a C-core, time-harmonic
b C-core, transient

algorithms available in iMOOSE, ILU(0) gives better performance than SSOR.

4 Discussion

The $\vec{A}-\vec{A},\ V$ formulation proves to be, as expected, best in terms of convergence stability over a wide range of frequencies and time-steps. For higher frequencies the $\vec{A}-\vec{A}^*$ formulation has advantages. It will compute the solution faster particularly due to the smaller number of unknowns. Nevertheless, the application is restricted to short-circuited eddy-current regions. Thus the $\vec{A}-\vec{A},V$ formulation is more versatile. The differences are less pronounced in the transient model. The $\vec{A}-\vec{A},\vec{T}$ formulation has poor numerical stability, especially in the transient model, where the system cannot be made symmetric and a BICG has to be used. Convergence is often not reached.

The $\vec{A}-\vec{A},\vec{T}$ formulation does have its advantages where an overall current is imposed in the eddy-current region.

5 Conclusions

Three formulations all based on the use of the magnetic vector potential and combined with either an electric scalar or vector potential have been presented, for both a time-harmonic and a transient model. The convergence behaviour is analysed for two different applications. The assumption of the $\vec{A}-\vec{A},V$ formulation being the best in terms of stability and convergence and the most versatile is confirmed. For special problems the $\vec{A}-\vec{A}^*$- or $\vec{A}-\vec{A},\vec{T}$ formulation gives better or faster results.

6 Acknowledgment

This article is dedicated to Prof. Gerhard Henneberger, who is released into his well deserved retirement with gratitude and appreciation for his meritorious scientific work.

7 References

1 Fujiwara, K., and Nakata, T.: 'Results for benchmark problem 7 (asymmetrical conductor with a hole)', *Compel*, 1990, **9**, (3), pp. 137–154

2 "Innovative modern object-oriented solving environment: iMOOSE," Available: http://www.imoose.de accessed March 2004

3 van Riesen, D., Monzel, C., Kaehler, C., Schlensok, C., and Henneberger, G.: 'iMOOSE: an open-source environment for finite-element calculations', *IEEE Trans. Magnetics*, 2004, **40**, (2), pp. 1390–1393

4 Bíró, O.: 'Edge element formulations of eddy-current problems', *Comput. Methods Appl. Mech. Eng.*, 1999, **169**, pp. 391–405

5 Kaehler, C., van Riesen, D., Albertz, D., and Henneberger, G.: 'Comparison of the $\vec{A}-\vec{A},\vec{T}$ and the $\vec{A}$ formulation for the computation of transient eddy-current field problems with edge elements', Proc. 10th Int. IGTE Symp. on Numerical Field Calculation in Electrical Engineering, Graz, Austria, 16–18 September 2002, p. 88

6 Zienkiewicz, O., and Taylor, R.: 'The finite-element method', (McGraw-Hill, London, 1989) Vol. 1

7 Albertz, D., and Henneberger, G.: 'On the use of the new edge-based $\vec{A}-\vec{A},\vec{T}$ formulation for the calculation of time-harmonic stationary and transient eddy-current field problems', *IEEE Trans. Magnetics.*, 1999, **36**, (4), pp. 818–822

8 Lahaye, D.: 'Algebraic multigrid for two-dimensional time-harmonic magnetic field computations'. PhD Dissertation, Katholieke Universiteit Leuven, Leuven, Belgium 2001